Capturing transient granular rheology with extended fabric tensor relations

manuscript No.
(will be inserted by the editor)

Capturing Transient Granular Rheology with Extended Fabric Tensor Relations

Eduardo Rojas Parra[1] · **Ken Kamrin**[2]

Received: date / Accepted: date

Abstract We present an improved continuum model for transient processes in granular simple shearing, which predicts the coupled evolution of the effective friction coefficient and fabric tensor. Specifically, the model gives the transient strength associated to the kinematics and the structure of the granular media for the quasi-static regime. The results of the continuum model were compared against molecular dynamic simulations. The comparison for the modulus and the angle of the principal directions of the fabric tensor showed a very good agreement for all the cases analyzed. The new fabric evolution model is capable of capturing the abrupt fall in the fabric modulus and in the effective friction coefficient at the beginning of reversal processes, when the network is destroyed. The model also predicts the right spin direction of the fabric angle, when the force chains move from one steady state to another, during reversal. Improvement in modeling the stress is obtained by relating the friction coefficient to the fabric and the unit shear rate tensors.

Keywords Granular materials · Transient rheology · Fabric tensor · Effective friction coefficient.

1 Introduction

Dense granular flows are the focus of enormous interest due their numerous applications in industrial and geophysical processes. Despite this, the behaviour of particle flows remains not totally understood and a general constitutive law to represent its behaviour has remained elusive. A crucial advance to elucidate this issue was to establish the inertial rheology for the case of quasi-rigid particles flowing steadily in a simple shear cell [1,2,3]. In this case it is possible to form just one dimensionless parameter called the 'inertial number' $I = d|\dot{\gamma}|/\sqrt{p/\rho_p}$, where d represents the mean diameter of the particles, $\dot{\gamma}$ corresponds to the shear rate, p is the confining pressure exerted by the walls and ρ_p is the mass density of the particles. Hence, output variables like the effective friction coefficient $\mu = |\sigma_{xy}|/p$, where σ_{xy} represents the shear component of the stress tensor $\boldsymbol{\sigma}$, as well as the volume packing fraction ϕ, are just functions of the inertial number, that is: $\mu(I)$ and $\phi(I)$.

Dense particle flows occur for $I \leq 0.1$, while the quasi-static flows are commonly assumed at $I \leq 10^{-4}$ [4]. The dense flows which are not quasi-static corresponds to the inertial regime where the rheology $\mu = \mu(I)$ was obtained. This inertial rheology and its extension to 3D (see [5]) have been intensively tested at the steady state condition. The test results show that the inertial rheology is not satisfied for inhomogeneous fields at low or moderate shear rate where non-local effects cannot be neglected [6,7,8]. The 3D extension to the inertial rheology, which assumes that stress and shear rate tensors remain aligned, is also not satisfied for some cases like rotating drums, but still the invariants of these two tensors are generally related well via the $\mu(I)$ relation in regions of faster flow [9].

On the other hand, transient processes for granular flows are not within the purview of these steady rheological models. There is a general agreement that the granular microstructure is important to modeling transient processes. While elasto-plastic and elasto-visco-plastic models have been adapted to introduce microstructure [10,11], there are some models that add a new and independent equation. These equations have been formulated in an incremental form for a so-called *anisotropy modulus* scalar variable as in [12,13], and also, in a differential form applied to the fabric tensor as in [14, 15,16,17,18].

1. Department of Mechanical Engineering, University of Antofagasta, Chile. E-mail: eduardo.rojas@uantof.cl ·
2. Department of Mechanical Engineering, Massachusetts Institute of Technology, USA. E-mail: kkamrin@mit.edu

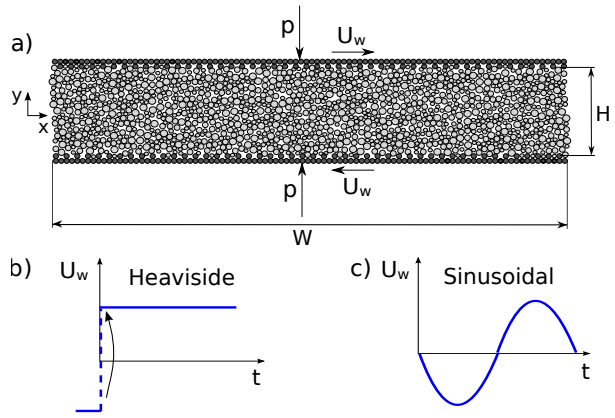

Fig. 1 (a) Numerical set-up. The height of the system is $H = 37d$ while the base width is $W = 4H$. The imposed wall velocities are: (b) Heaviside reversal and (c) sinusoidal reversal.

In this study, a general continuum model is presented for unsteady state shear processes in a dense granular medium. The model assumes that during transients, the granular structure, represented by the fabric tensor, changes according a differential evolution equation. Also, we establish a relationship between the stresses, specifically the effective friction coefficient μ, and the structure. We rooted our work in relationships obtained previously in [15]. Important changes were made to obtain improved accuracy, and we applied stringent shear reversal tests as part of our validation to achieve better qualitative and quantitative agreement between continuum and discrete simulations.

2 Numerical set-up

The numerical experiment consists of a two-dimensional dry granular medium confined between two rough walls in the absence of gravity. The medium is made of a polydisperse mixture of circular grains with uniform mass density and diameters that are uniformly distributed in the range $[0.5d, 1.5d]$, where d is the average diameter. This distribution allows the system to have stable mixtures that do not present segregation or crystallization. The walls are made of particles of diameter d, which are forced to move at imposed velocities $\pm U_w$ to produce a Couette flow. The pressure p on the walls was controlled in order to keep it constant during the transient process. The height of the system was $H = 37d$ while the base width was $W = 4H$.

The transient is achieved by changing the velocity of the walls in two ways: (a) an instantaneous reversal of the velocity or Heaviside signal and (b) a sinusoidal signal. Thereby we impose a shear rate in the media that is a function of time $\dot{\gamma}(t)$. The inertial number I was the order of 10^{-4}, small enough to ensure the quasi-static regime.

The discrete element method (DEM) used in this work considers a usual contact model, where normal and tangential elastic forces are linear with elastic constants k_n and k_t, respectively. The spring constant for the normal force is set to obtain an overlap of the particles $\delta = 2 \cdot 10^{-5} d$, ensuring we remain in the hard particle limit. The tangential spring constant is fixed to $k_t = 0.5 k_n$ and the dissipative terms are fixed to obtain a restitution coefficient $e = 0.5$ for the collision between two particles of diameter d. The Coulomb friction coefficient is chosen equal to $\mu_p = 0.45$. The simulations were running using the YADE discrete element code [19].

3 Model

Below, we present a contact network dependent model for the stress ratio specialized for shear dominated flows. A generalization that includes volumetric effects is discussed briefly thereafter. The network is represented by the fabric tensor obtained from the unit contact vectors between particles. As the contact structure during the transient evolves, we also included an evolution equation for the fabric, which represents a relationship between fabric, shear rate and spin tensors. We defined the (deviatoric) fabric tensor as the symmetric traceless second order tensor:

$$\mathbf{A} = -\frac{1}{2}\mathbf{I} + \frac{1}{N_c}\sum_{c\in V} \mathbf{n}\otimes\mathbf{n}, \tag{1}$$

where $\mathbf{n}$ is the unit contact vector and N_c corresponds to the number of contacts c inside of the volume V. We denote the strain-rate tensor by $\mathbf{D} = \frac{1}{2}\left(\nabla\mathbf{v} + (\nabla\mathbf{v})^T\right)$, the spin tensor by $\mathbf{W} = \frac{1}{2}\left(\nabla\mathbf{v} - (\nabla\mathbf{v})^T\right)$, where $\mathbf{v}$ corresponds to the velocity field. For a 2D system, the deviatoric part of the shear rate tensor is given by $\mathbf{D}' = \mathbf{D} - \frac{1}{2}\mathbf{tr}(\mathbf{D})\mathbf{I}$. In our DEM simulations the vertical gradient of the vertical velocity associated to dilation was essentially noise around zero, hence we consider: $\mathbf{D} \approx \mathbf{D}' \approx 0.5\dot{\gamma}(\hat{\mathbf{i}}\otimes\hat{\mathbf{j}} + \hat{\mathbf{j}}\otimes\hat{\mathbf{i}})$.

3.1 Friction model

We find, from the molecular dynamics simulations, that there is not a one-to-one relationship between the (signed) stress ratio σ_{xy}/p and the off-diagonal fabric component in the presence of shear reversals (see Fig. 2.a). Better agreement is achieved by relating $\mu = |\sigma_{xy}|/p$ with a new variable $X = \mathbf{A} : \mathbf{D}'/|\mathbf{D}'|$ (see Fig. 2.b). Here, colon corresponds to the inner product defined for tensors (e.g. $\mathbf{M} : \mathbf{N} = M_{ij}N_{ij}$), and $|\cdot|$ represents tensorial modulus (e.g. $|\mathbf{M}| \equiv \sqrt{\mathbf{M} : \mathbf{M}}$). This new variable represents the component of $\mathbf{A}$ in the direction of $\mathbf{D}'$ and it is negative at steady state because these tensors are almost proportional but point in opposite directions. Also, at steady state, one of the principal directions of $\mathbf{A}$ is parallel to the average direction of force chains. In this study, we are

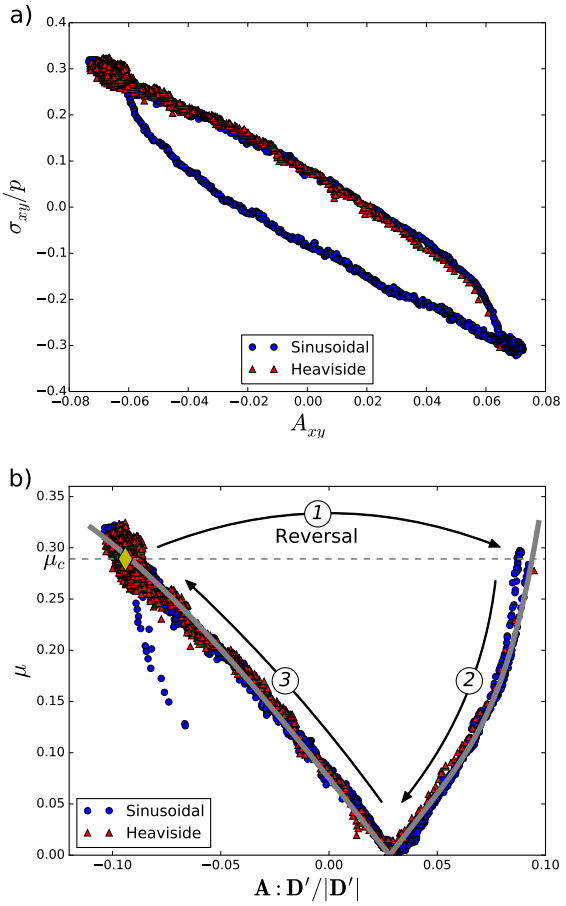

Fig. 2 Effective friction coefficient μ versus fabric (from DEM simulations). a) Signed stress ratio σ_{xy}/p versus the xy component of the fabric tensor, A_{xy}. b) μ versus $X = \mathbf{A}:\mathbf{D}'/|\mathbf{D}'|$. The yellow point corresponds to the steady state condition. Solid gray line represents the fit $\mu(X)$ given in equation (2).

going to consider this principal direction θ_A as the direction of $\mathbf{A}$ (measured counterclockwise respect to the x axis).

Figure 2.b shows the sequence of the transient process for both Heaviside and sinusoidal strain rate reversals. Here, the yellow point represents the steady state condition before the reversal. As the inertial number tends to zero for the entire process, the steady state effective friction coefficient takes the threshold value $\mu_c = \mu(I \cong 0)$. When the strain changes its direction, the reversal occurs and the variable X becomes instantaneously positive (reversal ①). In this moment, the fabric and the shear rate tensors point for one instant in the same direction. This condition generates compression perpendicular to the force chains, starting a fast process of grain network destruction, which causes the strength to decay (trajectory ②). Finally, there is a slower process where the effective friction coefficient comes back to its steady value and the force network reaches a new steady state direction, perpendicular to the previous one (trajectory ③).

The fit $\mu(X)$ for the curve showed in Fig.2.b, constitutes the model for μ written below as a function of $y(X) = X - 0.028$:

$$\mu(X) = \begin{cases} -2.7\,y(X) + 20\,y(X)^3 & , y(X) < 0 \\ 2.7\,y(X) + 9.0\cdot 10^4\,y(X)^5 & , y(X) \geq 0. \end{cases} \tag{2}$$

The $\mu = \mu(X)$ relationship in our model replaces the quadratic form of the similar variable $\eta = a_1 + a_2 X + a_3 X^2$ from [15], where the a_i are constant values. Indeed, the variable X has some beneficial characteristics for the analysis at hand: it is dimensionless, it is shear rate direction independent at steady state, and it is independent of shear-rate magnitude.

Assuming that the deviatoric part of the stress and the strain rate are aligned, it is possible to write a generalized friction law:

$$\boldsymbol{\sigma}' = \frac{\mu(X)p}{\sqrt{2}}\frac{\mathbf{D}'}{|\mathbf{D}'|}. \tag{3}$$

The shear-specialized formulation we have presented above is not valid when the system is static or when the strain-rate deviator is otherwise null. In these cases, the shear stress $\boldsymbol{\sigma}'$ could be equal to the null tensor, but $\boldsymbol{\sigma}'$ also could be finite, given by a solid-like model such as elasticity [20,21], which is beyond of the objectives of this work. Equation (3) would also not apply in isotropic compression/extension, where the shear stress $\boldsymbol{\sigma}'$ and the deviator of the shear rate tensor $\mathbf{D}'$ are null, but $\mathbf{D}$ is not. In this particular case, one option is to consider a modified model as in [15] where $\boldsymbol{\sigma}' = \frac{\eta p}{\sqrt{2}}\frac{\mathbf{D}'}{|\mathbf{D}|}$. The scalar variable η is related to the effective friction coefficient via the modulus of $\mathbf{D}$ and $\mathbf{D}'$, but both μ and η should be very similar in shear-dominated flow, i.e. $\eta = \mu\frac{|\mathbf{D}|}{|\mathbf{D}'|} \approx \mu$.

3.2 Fabric tensor model

We assume that the fabric tensor is governed by an independent evolution equation during the transient with the following form:

$$\overset{\triangledown}{\mathbf{A}} = \Psi(\mathbf{A},\mathbf{D}') \equiv \alpha_1\mathbf{D}' + \alpha_2|\mathbf{D}'|\mathbf{A}, \tag{4}$$

where $\overset{\triangledown}{\mathbf{A}} = \dot{\mathbf{A}} + \mathbf{A}\mathbf{W} - \mathbf{W}\mathbf{A}$ is the *Jaumann Rate* and $\dot{\mathbf{A}}$ is the material time derivative of $\mathbf{A}$. The Jaumann or co-rotational rate, in contrast with the material time derivative, is a frame-indifferent tensorial rate, which vanishes for all rigid-body motions of the material. The function for Ψ shown above on the right-hand side was arrived at by first applying a well-known representation theorem for symmetric tensors [22], which limits the possible ways Ψ can depend on its inputs. We then keep only the lowest order terms in this expansion

i	a_i	b_i	c_i	d_i
1	-1.8	0	21	1.5
2	-9.0	100	-900	2.0

Table 1 Fitting parameters for the coefficients α_i of the equation (6).

and, in accord with the theorem, allow the scalar prefactors for each term to depend only on joint scalar invariants of $\mathbf{A}$ and $\mathbf{D}'$. By expressing those prefactors as α_1 and $\alpha_2|\mathbf{D}'|$, as shown above, where the $\alpha_{1,2}$ are functions of only rate-independent invariants, the entire evolution model is assured to be rate independent.

In general, the first term on the right side of equation (4) pushes the fabric to grow in the direction of principal compression of the flow, while the second one opposes its growth and eventually stops the fabric evolution under continual shearing, admitting a steady fabric state. In this equation, if the coefficients α_i are chosen as $\alpha_1 = c_1$ and $\alpha_2 = c_2 + c_3(\mathbf{A} : \mathbf{D}')/|\mathbf{D}|$, where c_i are constant values, and if we consider that $|\mathbf{D}|$ is approximately $|\mathbf{D}'|$ in our shear flows, we arrive at the same equation in [15] for the fabric deviator, i.e.

$$\overset{\triangledown}{\mathbf{A}} = c_1\mathbf{D}' + c_2|\mathbf{D}|\mathbf{A} + c_3(\mathbf{A} : \mathbf{D}')\mathbf{A}. \tag{5}$$

Using the information available from DEM simulations, we solved equation (4) considering the coefficients α_i as unknowns for two kinds of shear reversal: Heaviside and sinusoidal. It was found that the coefficients of the evolution equation are not constants but are rather well-represented as a single function of the new variable $X = \mathbf{A} : \mathbf{D}'/|\mathbf{D}'|$, noting that X is a valid, joint scalar invariant of $\mathbf{A}$ and $\mathbf{D}'$. Figure 3 shows two regions where the coefficients α_i behave in a different way. The right side of region B represents the beginning of the reversal, while region A represents a zone near the steady state (points where $X < -0.05$ were omitted because of the noise of the results in this zone). In region A α_1 was fitted as a negative constant value, while α_2 was fitted as a linear function of X. Region B is noisy but the coefficients clearly show a strong tendency to decrease for α_1 and increase for α_2 until point $X_0 = 0.0827$, where both coefficients diverge. The fit functions we choose for α_i are:

$$\alpha_i = \begin{cases} a_i + b_i X & , X \leq 0 \\ a_i + b_i X + c_i \frac{X^{d_i}}{X - X_0} & , X > 0, \end{cases} \tag{6}$$

where the constant parameters involved are shown in Table 1. Note the function is continuous and differentiable at $X = 0$. Figure 3 also shows the best fits found for the evolution model given in [15] (see equation 5).

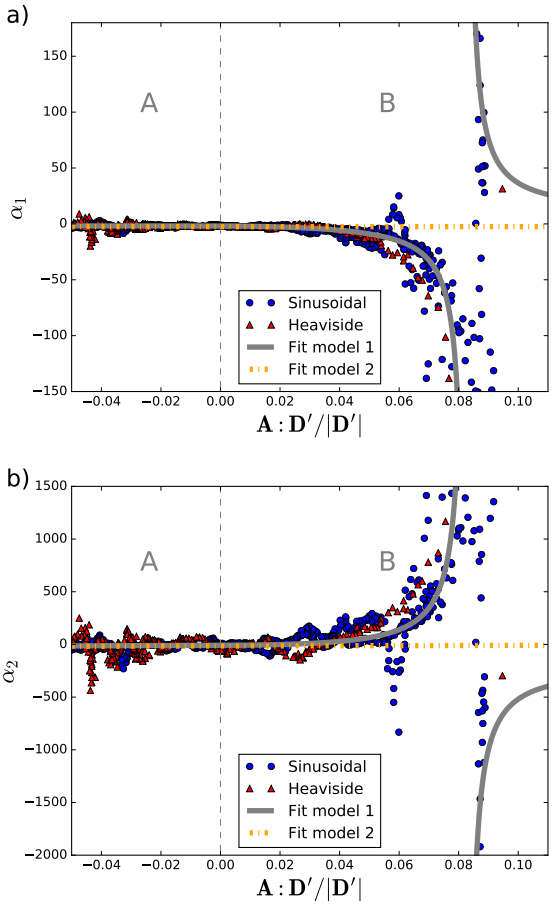

Fig. 3 Coefficients α_i obtained from equation (4). Solid gray line represents the fit considered in this work (Model 1), while dashed orange line represents the model given in [15] (Model 2). a) α_1 versus $X = \mathbf{A} : \mathbf{D}'/|\mathbf{D}'|$. b) α_2 versus $X = \mathbf{A} : \mathbf{D}'/|\mathbf{D}'|$.

4 Results

We solved the fabric evolution equation numerically for the model presented in this work (Model 1) and for the previous one given in [15] (Model 2), by using the fourth-order Runge-Kutta method. For both cases, equation (2) was used to obtain the shear stress ratio μ. We expressed the fabric tensor in terms of its modulus $|\mathbf{A}|$ and the angle of its major principal vector $\theta_{\mathbf{A}}$, which corresponds to the compression direction of the force chains.

Figure 4 and 5 show the results for the fabric tensor models and the effective friction coefficient μ, in comparison with DEM simulations, for an imposed Heaviside and sinusoidal reversal, respectively. Both Model 1 and 2 present a good agreement with DEM simulation for $|\mathbf{A}|$. However, in general Model 1 captures more accurately the very strong fall just after the reversal. The transient of the fabric angle is not captured for the previous model and turns in the opposite direction in some cases. Instead, the data shows the fabric angle always passes through a vertical orientation, which

the new model captures and it is attributed to the more robust fit of the coefficients α_i when the variable X is in zone B of the figure 3. The sinusoidal shear test shows that the width of the transition in θ_A during reversal is too sharp in Model 2, and is closer to the data in the new model. Finally, the correlation presented in equation 2 for μ is shown to do a better job at the beginning of the reversal process where the change in μ happens very quickly (see zoom-in inserted in Fig 4.c).

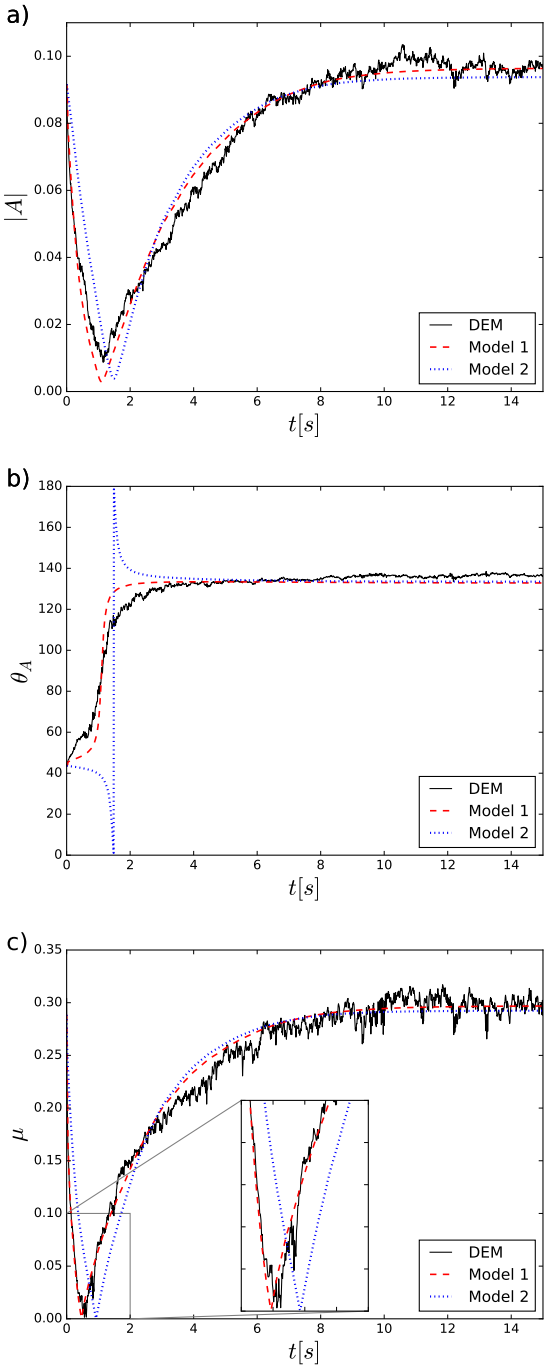

Fig. 4 Results for the Heaviside reversal case. Solid black line represents DEM simulation results, dashed red line results obtained using the model developed in this work (Model 1), while dotted blue line results obtained using the model given in [15] (Model 2).

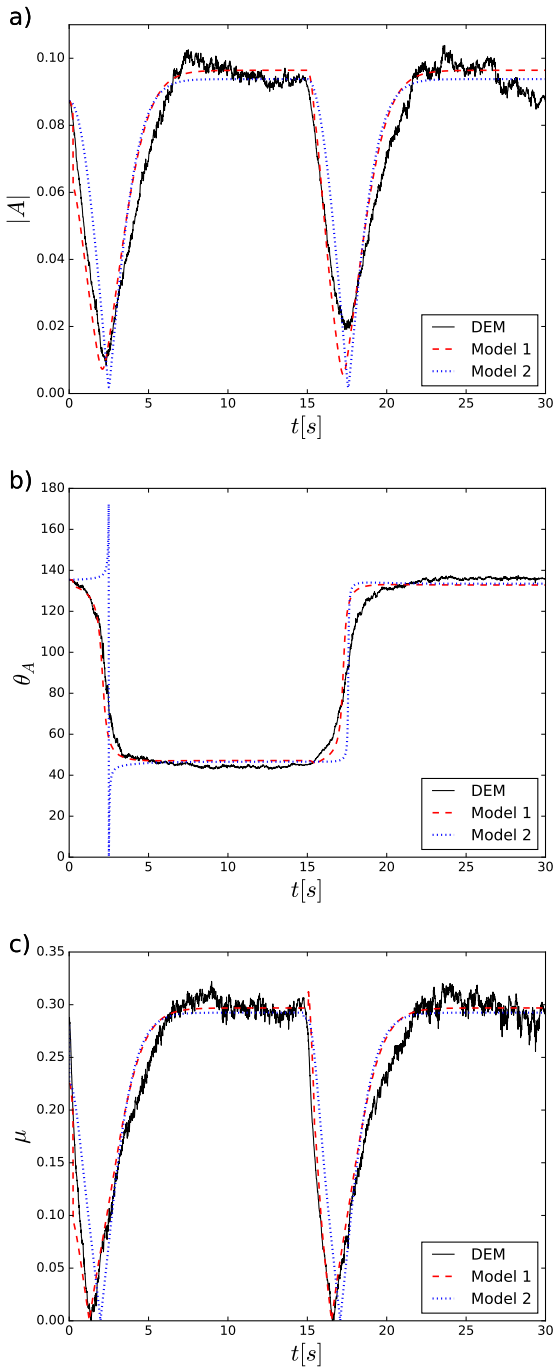

Fig. 5 Results for the sinusoidal reversal case. Solid black line represents DEM simulation results, dashed red line results obtained using the model developed in this work (Model 1), while dotted blue line results obtained using the model given in [15] (Model 2).

5 Conclusion

In this paper, the rheology for unsteady dry granular flows in a Couette cell is studied in the quasi-static limit. We found that the rheology in this case depends on the structure of the granular medium represented by the fabric tensor, $\mathbf{A}$. We found that the effective friction coefficient μ is a one-to-one function of the fabric tensor contracted with the shear rate tensor direction, $X = \mathbf{A} : \mathbf{D}'/|\mathbf{D}'|$.

We have presented an improved evolution equation to predict the fabric tensor behaviour and friction evolution during the transient, including coefficients that depend on the structure through the variable X. This offers certain improvements over a previous model proposed in [15]. The model is capable of capturing the abrupt fall in the fabric modulus and in the effective friction coefficient just after flow reversal, when the network is destroyed and the medium becomes almost isotropic. During this starting lapse of time, the angle of the fabric changes its direction to the opposite steady state value in a soft way. This behaviour is well predicted by our non-constant coefficient model but not captured as well by preceding ones. Aside from predicting the effective friction, our new improvement to the fabric evolution could be useful in problems where the network orientation plays a direct role in some physical phenomenon, e.g. in determining macroscopic conductivity in flowing granular systems of conductive particles, or in predicting anisotropic passage of pressure waves. However, the new fabric model is very sensitive to small changes in the coefficients. This could be related to the fact that the coefficients diverge at $X = X_0$, necessitating high accuracy numerical integration.

Acknowledgements

ER would like to acknowledge support from Comisión Nacional de Investigación Cientfica y Tecnológica. KK acknowledges support from NSF grant CBET-1706193.

Compliance with ethical standards

Conflict of interest The authors declare that they have no conflict of interest.

References

1. MiDi, G. D. R. (2004). On dense granular flows. The European Physical Journal E, 14(4), 341-365.
2. Jop, P., Forterre, Y., & Pouliquen, O., Nature (London) 441, 727 (2006). Nature (London), 441, 727.
3. Da Cruz, F., Emam, S., Prochnow, M., Roux, J. N., & Chevoir, F. (2005). Rheophysics of dense granular materials: Discrete simulation of plane shear flows. Physical Review E, 72(2), 021309.

4. DeGiuli, E., McElwaine, J. N., & Wyart, M. (2016). Phase diagram for inertial granular flows. Physical Review E, 94(1), 012904.
5. Jop, P. (2008). Hydrodynamic modeling of granular flows in a modified Couette cell. Physical Review E, 77(3), 032301.
6. Aranson, I. S., Tsimring, L. S., Malloggi, F., & Clément, E. (2008). Nonlocal rheological properties of granular flows near a jamming limit. Physical Review E, 78(3), 031303.
7. Kamrin, K., & Koval, G. (2012). Nonlocal constitutive relation for steady granular flow. Physical review letters, 108(17), 178301.
8. Bouzid, M., Trulsson, M., Claudin, P., Clément, E., & Andreotti, B. (2013). Nonlocal Rheology of Granular Flows across Yield Conditions. Physical Review Letters, 111(23), 238301.
9. Cortet, P. P., Bonamy, D., Daviaud, F., Dauchot, O., Dubrulle, B., & Renouf, M. (2009). Relevance of visco-plastic theory in a multidirectional inhomogeneous granular flow. EPL (Europhysics Letters), 88(1), 14001.
10. Einav, I. (2012). The unification of hypo-plastic and elasto-plastic theories. International Journal of Solids and Structures, 49(11-12), 1305-1315.
11. Babeyko, A. Y., & Sobolev, S. V. (2008). High-resolution numerical modeling of stress distribution in visco-elasto-plastic subducting slabs. Lithos, 103(1-2), 205-216.
12. Luding, S., & Perdahcıoğlu, E. S. (2011). A local constitutive model with anisotropy for various homogeneous 2D biaxial deformation modes. Chemie Ingenieur Technik, 83(5), 672-688.
13. Kumar, N., Imole, O. I., Magnanimo, V., & Luding, S. (2014). Effects of polydispersity on the micromacro behavior of granular assemblies under different deformation paths. Particuology, 12, 64-79.
14. Goddard, J. D. (2006). A dissipative anisotropic fluid model for non-colloidal particle dispersions. Journal of Fluid Mechanics, 568, 1-17.
15. Sun, J., & Sundaresan, S. (2011). A constitutive model with microstructure evolution for flow of rate-independent granular materials. Journal of Fluid Mechanics, 682, 590-616.
16. Zhu, H., Mehrabadi, M. M., & Massoudi, M. (2006). Incorporating the effects of fabric in the dilatant double shearing model for planar deformation of granular materials. International journal of plasticity, 22(4), 628-653.
17. Sun, J., & Sundaresan, S. (2013). Radial hopper flow prediction using a constitutive model with microstructure evolution. Powder technology, 242, 81-85.
18. Olsen, T., Helal, A., McKinley, G. H., & Kamrin, K. (2016). Coupled dynamics of flow, microstructure, and conductivity in sheared suspensions. Soft matter, 12(36), 7688-7697.
19. Šmilauer et al. (2015). Yade Documentation 2nd ed. The Yade Project. DOI 10.5281/zenodo.34073 (http://yade-dem.org/doc/).
20. Kamrin K. (2010) Nonlinear elasto-plastic model for dense granular flow. International Journal of Plasticity. 1;26(2):167-88.
21. Dunatunga S., & Kamrin K. (2015) Continuum modelling and simulation of granular flows through their many phases. Journal of Fluid Mechanics, Sep;779:483-513.
22. Rivlin, R. S. (1955) Further remarks on the stressdeformation relations for isotropic materials, Journal of Rational Mechanics and Analysis, 4(5), 681702.